New Delhi Metallo-β-Lactamase: Structural Insights into β-Lactam Recognition and Inhibition

Dustin T. King, Liam J. Worrall, Robert Gruninger, and Natalie C. J. Strynadka*

Department of Biochemistry and Molecular Biology and Center for Blood Research, University of British Columbia, 2350 Health Sciences Mall, Vancouver, British Columbia, Canada V6T 1Z3

S *Supporting Information*

ABSTRACT: The β-lactam antibiotics have long been a cornerstone for the treatment of bacterial disease. Recently, a readily transferable antibiotic resistance factor called the New Delhi metallo-β-lactamase-1 (NDM-1) has been found to confer enteric bacteria resistance to nearly all β-lactams, including the heralded carbapenems, posing a serious threat to human health. The crystal structure of NDM-1 bound to meropenem shows for the first time the molecular details of how carbapenem antibiotics are recognized by dizinc-containing metallo-β-lactamases. Additionally, product complex structures of hydrolyzed benzylpenicillin-, methicillin-, and oxacillin-bound NDM-1 have been solved to 1.8, 1.2, and 1.2 Å, respectively, and represent the highest-resolution structural data for any metallo-β-lactamase reported to date. Finally, we present the crystal structure of NDM-1 bound to the potent competitive inhibitor L-captopril, which reveals a unique binding mechanism. An analysis of the NDM-1 active site in these structures reveals key features important for the informed design of novel inhibitors of NDM-1 and other metallo-β-lactamases.

β-Lactams such as the penicillins and carbapenems constitute ~50% of all antibiotic prescriptions worldwide.[1] These antibacterials inhibit cell wall biosynthesis by acting as substrate analogues to prevent transpeptidase-mediated cross-linking of adjacent peptidoglycan strands.[2] The prospect that bacteria can develop or acquire high levels of resistance to these and other antibiotics is a global health concern. The most prevalent cause of bacterial resistance to β-lactam antibiotics is the expression of β-lactamase enzymes, which hydrolyze the amide bond in the β-lactam ring, yielding an inactivated product.[3]

β-Lactamase enzymes consist of four classes (A−D) based upon DNA sequence similarity. Classes A, C, and D utilize an active-site serine as a nucleophile, whereas the class-B enzymes are metallo-β-lactamases (MBLs), which use active-site zinc to coordinate a nucleophilic hydroxide to mediate hydrolysis. The class-B enzymes are further divided into subclasses B1, B2, and B3, of which the class-B1 enzymes have emerged as the most clinically significant and are characterized as having two active-site zinc ions (Figure 1).[3,4]

There has been little advance in the development of clinically relevant MBL inhibitors.[5] Among the most promising candidates are the L and D diastereomers of the mercapto-carboxamide inhibitor captopril, which display potent and
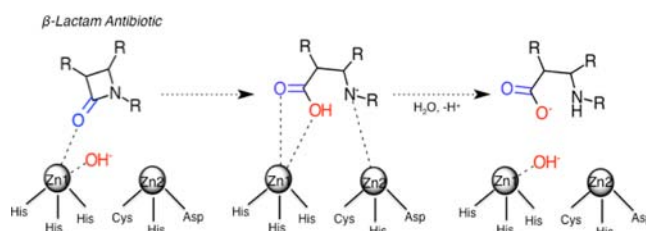

Figure 1. β-Lactam hydrolysis mediated by class-B1 metallo-β-lactamases.

broad-spectrum MBL inhibitory activity.[6] L-Captopril is an FDA-approved angiotensin-converting enzyme (ACE) inhibitor used clinically to treat hypertension.

Recently, a novel class-B1 MBL called New Delhi metallo-β-lactamase-1 (NDM-1) was found to confer enteric bacteria with nearly complete resistance to all β-lactam antibiotics, including the late-generation carbapenems meropenem and imipenem.[7] This activity is of particular concern as carbapenems have the widest spectrum of activity of all the β-lactam antibiotics and are used clinically as our last line of defense against multi-drug-resistant Gram-negative bacteria, in particular those displaying extended-spectrum β-lactamase activity.[8] Additionally, NDM-1 is encoded on a readily transferable plasmid, which facilitates its transmission.[7] NDM-1 has spread to nearly every continent worldwide and has become a formidable threat to human health, prompting the World Health Organization to issue a global warning.[9,10] To gain insight into β-lactam recognition and inhibition, we used X-ray crystallography to characterize NDM-1 bound to various β-lactams as well as to the potent inhibitor L-captopril, the latter representing the first reported structure for an NDM-1−inhibitor complex.

Crystal structures of hydrolyzed methicillin-, benzylpenicillin-, oxacillin-, and meropenem-bound NDM-1 were solved to 1.2, 1.8, 1.2, and 1.9 Å, respectively. The penicillin and meropenem product complexes crystallized in the space groups $P2_12_12_1$ and $P4_12_12$, respectively, with two protein chains in the asymmetric unit [Table S1 in the Supporting Information (SI)]. There are two zinc ions displaying clear $F_o − F_c$ electron density in each active site, which were refined at 90% occupancy and confirmed previously by inductively coupled plasma mass spectrometry and anomalous X-ray diffraction data collected at the zinc edge.[12] The two chains in the asymmetric unit display high structural similarity [with root-mean-square
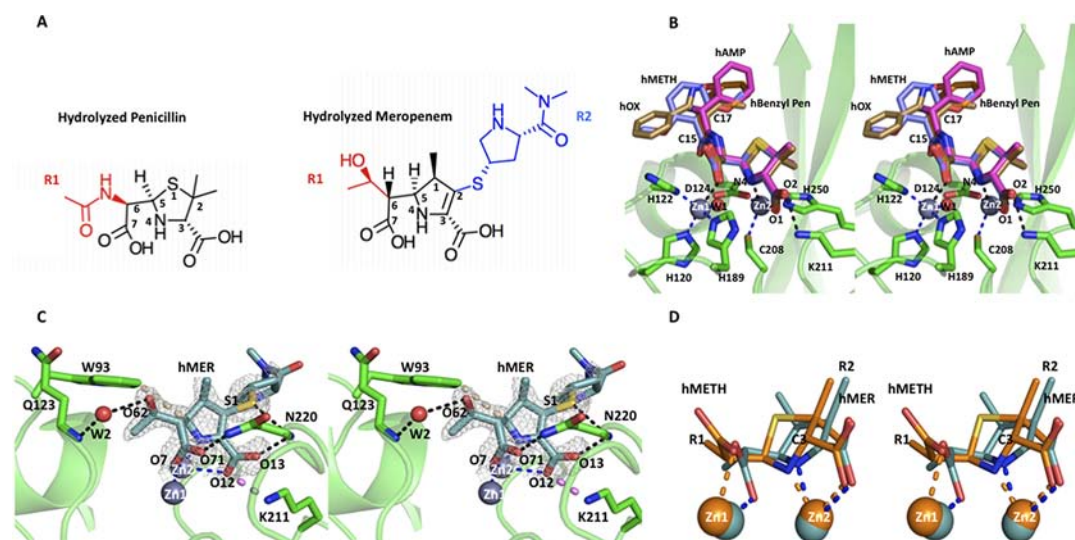
Figure 2. Crystal structures of β-lactam product complexes. (A) Structures of hydrolyzed penicillin and hydrolyzed meropenem (hMER). (B) Overlay of penicillin product complexes bound to NDM-1. The carbon atoms of hydrolyzed benzylpenicillin (hBenzyl), hydrolyzed ampicillin (hAMP, PDB entry 3Q6X),[11] hydrolyzed methicillin (hMETH), and hydrolyzed oxacillin (hOX) are shown in orange, pink, slate, and brown, respectively; other atoms are colored by type (N, blue; O, red; S, yellow). The NDM-1 structure is represented as a green ribbon, and zinc coordinating ligands are shown as green sticks with non-carbon atoms colored by type. (C) Structure of hMER-bound NDM-1. NDM-1 is shown as a green ribbon with selected active-site residues displayed as green sticks with non-carbon atoms colored by type. The hMER ligand is slate with non-carbon atoms colored by type, and the $2F_o - F_c$ electron density is contoured to 0.9σ and represented as a gray mesh. Zinc ions are shown as gray spheres. (D) hMER/hMETH overlay close-up of zinc coordination. hMETH and hMER are shown as orange and slate sticks, respectively, with non-carbon atoms colored by type. Zinc ions are slate and orange spheres for the hMER- and hMETH-bound structures, respectively. In (B−D), bonds representing zinc coordination, hydrogen bonding, and hydrophobic and electrostatic interactions are displayed as thin blue, thin black, thick gray, and thick purple dashes, respectively.

deviations (RMSDs) of 0.1, 0.2, 0.1, and 0.8 Å for all common alpha-carbon (CA) atoms in chains A and B for hydrolyzed methicillin-, benzylpenicillin-, oxacillin-, and meropenem-bound NDM-1, respectively], and therefore, we limited our analysis to chain A for each product complex. All of the hydrolyzed β-lactam products display clear $2F_o - F_c$ electron density in the dizinc-containing active sites of both protein chains in the asymmetric unit; the penicillin complexes (Figure S1 in the SI) were refined at full occupancy and the hydrolyzed meropenem structure (Figure 2C) at 0.8 occupancy.

The observed position of the presumed nucleophilic hydroxide, W1, is common to all of the penicillin product complex structures and is located directly between Zn1 and Zn2 at distances of 2.0 ± 0.1 and 3.0 ± 0.1 Å, respectively. Previously, it was thought that following product release W1 is reloaded between the zinc ions for another round of hydrolysis.[13,4] However, the presence of the nucleophilic W1 in our product complexes leads us to propose that for hydrolysis of the penicillins, the nucleophilic hydroxide may be reloaded into its catalytic position even before the product leaves the active site. This proposition is in keeping with pre-steady-state kinetic data suggesting that the rate-limiting step in NDM-1- and CcrA-mediated nitrocefin hydrolysis is protonation of the nitrogen leaving group after C−N bond scission rather than reloading of the nucleophile.[14,15] However, to elucidate fully the detailed mechanistic features of hydrolysis, further pre-steady-state kinetic studies are required.

Penicillins are drug variants that contain a five-membered thiazolidine ring fused to the β-lactam ring moiety (Figure 2A). Atoms within this penicillin core displayed lower average temperature factors than those within the side R1 functional group when averaged across all of the hydrolyzed products (9.7 vs 15.0 Å^2). In addition, the R1 functional group displays variable conformations, while the β-lactam core is virtually identical in all of the product complexes analyzed (RMSD of 0.1 Å on all common penicillin core atoms) (Figure 2B). Thus, the penicillin core coordinates to the NDM-1 zinc center in a precise and rigid conformation that is independent of the constituents present on the R1 functional group. Remarkably, we see that the enlarged NDM-1 active-site cleft easily accommodates the bulky methicillin and oxacillin R1 groups located directly between the L3 and L10 loops (Figure S1). The fact that NDM-1 accommodates bulky R1 groups suggests that addition of large moieties at this position (historically the typical site of change for creation of new β-lactam variants) may not be an effective strategy for the design of novel NDM-1-resistant β-lactams.

In all structures, Zn1 is bound 2.5 Å away from the C6 carboxylate oxygen of the substrate. Zn2 displays tight binding to N4 and the C3 carboxylate oxygen at 2.1 and 2.2 Å, respectively (Figure 2B). Recently, the monobactam antibiotic aztreonam has been characterized as the only β-lactam that is poorly hydrolyzed by NDM-1.[15] Monobactams are characterized by the absence of a fused ring attached to the β-lactam core. Consequently, monobactams lack the C3 carboxylate that is present in all other classes of β-lactam antibiotics and is required for interaction with one or both hydroxyl groups within the penicillin binding protein (PBP) transpeptidase active-site KTGT motif as well as for electrostatic interaction with proximal conserved Lys/Arg side chains.[2] Instead, monobactams have a bulky electronegative sulfate group covalently attached to N4 that binds the conserved PBP KTGT motif.[16] Our high-resolution structures of NDM-1−penicillin product complexes display a particularly strong coordination interaction between the C3 carboxylate and Zn2 (Figure 2B), suggesting a potential reason why aztreonam,

lacking this carboxylate, is poorly hydrolyzed by this enzyme. Modeling of aztreonam in the NDM-1 active site suggests that the sulfate, which is displaced effectively one carbon unit from the carboxylate, is too far away (~3.5 Å) for direct coordination to Zn2 and has overall weakened electrostatic interactions to the enzyme active site (Figure S4). Therefore, the development of the monobactams presents a logical avenue for the design of novel antibiotics that are not recognized by MBLs.

The hydrolyzed carbapenem core of meropenem displays extensive noncovalent interactions with the zinc center, but the pyrrolidine *N,N*-dimethylcarboxamide (DMP) R2 group does not exhibit any strong interactions with NDM-1 (Figure S2). Indeed, the carbapenem core was refined with lower average temperature factors than the DMP group (31.2 ± 5.1 vs 55.0 ± 6.5 Å^2). This observed disorder may be in part responsible for the higher K_m values of NDM-1 for meropenem (49.0 μM) than for benzylpenicillin (22.0 μM) and ampicillin (16.0 μM).[17] However, the large NDM-1 active-site cleft provides steric accommodation of the bulky DMP functional group despite the lack of specific interactions, leading to recognition and hydrolysis of meropenem. We therefore conclude that simple functionalization of the carbapenem R2 group may not be an effective strategy for the design of novel MBL-resistant β-lactam antibiotics.

The carbapenem and penicillin cores bind differentially to the NDM-1 dizinc center. The carbapenem N4 and C3 carboxylate oxygen coordinate to Zn2 at 2.4 and 2.7 Å, respectively, in an analogous fashion to the hydrolyzed penicillin product complex structures (Figure 2D). However, the newly formed C6 carboxylate directly intercalates Zn1 and Zn2 at 2.2 and 2.6 Å, respectively, and acts as a bridging coordination ligand, resulting in tetrahedral coordination of Zn1 and hexacoordination of Zn2 in the product complex. This differs from the hydrolyzed penicillin-bound structures, in which the C6 carboxylate is shifted away from Zn2 toward the L10 loop, resulting in penta- rather than hexacoordination of Zn2 (Figure 2D). Also, the interzinc distance in the meropenem-bound structure (4.0 Å) is shorter than in the penicillin product complex structures (4.6 Å). However, despite these conformational differences, the NDM-1-mediated hydrolyses of meropenem, benzylpenicillin, and ampicillin display remarkably similar K_{cat} values (12, 11, and 15 s^{-1}, respectively).[17] The observed variability in binding of the penicillin and carbapenem cores in NDM-1 exemplifies the ability of zinc to facilitate multiple ligand geometries and coordination numbers.[18]

It has been suggested that the highly conserved N220 of class-B1 MBLs contributes to the formation of an oxyanion hole and stabilizes the tetrahedral intermediate via interaction between its δNH$_2$ and the lactam carbonyl oxygen O71.[19,4] For the homologue IMP-1 (32% identity), the N220A and N220E mutants displayed significantly increased K_m and reduced K_{cat} values for hydrolysis of imipenem relative to the wild-type, supporting an important role for N220 in carbapenem binding and hydrolysis.[20] In the meropenem product complex structure, the C6 carboxylate oxygen O71 displays tight hydrogen bonding to the δNH$_2$ side-chain nitrogen of N220 (2.8 Å; Figure 2C and Figure S5). These results provide evidence that N220 interacts directly with the substrate and thus support the potential role of this residue in stabilizing the transient tetrahedral intermediate via formation, along with Zn1, of an oxyanion hole.

Previously, the crystal structure of the class-B1 MBL enzyme BlaB from *Chryseobacterium meningosepticum* in complex with D-captopril was solved to 1.5 Å resolution.[6] Here we present the first reported crystal structure of an L-captopril-inhibited MBL enzyme complex to 2.4 Å resolution. The L-captopril bound NDM-1 crystals are $P4_12_12$ with two protein chains in the asymmetric unit. The two chains display high overall structural similarity (RMSD of 0.2 Å on all common CA atoms within chains A and B), and therefore, only chain A was used for structural analysis.

The L-captopril S1 atom intercalates directly between Zn1 and Zn2, 2.1 Å from both ions. Upon binding, S1 displaces the nucleophilic W1, leading to a competitively inhibited enzyme. In this complex, both Zn1 and Zn2 display tetrahedral coordination geometries in which the L-captopril S1 occupies the fourth coordination site for each ion (Figure 3B). The
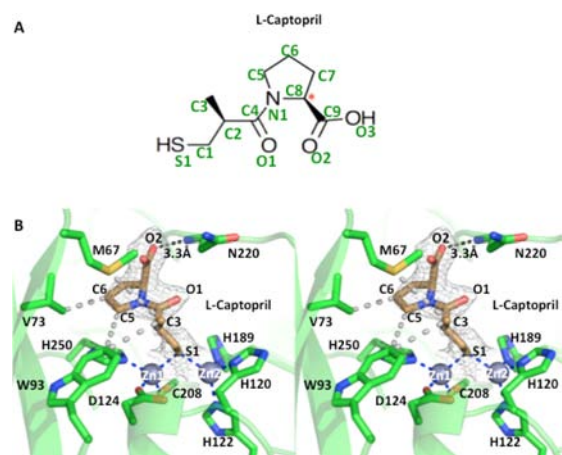

Figure 3. Competitive inhibition of NDM-1 by captopril. (A) Structure of L-captopril. The chiral carbon is highlighted with a red asterisk. (B) Structure of L-captopril-bound NDM-1. The NDM-1 backbone is represented as a green ribbon, and selected active-site residues are shown as green sticks with non-carbon atoms colored by type. The L-captopril ligand is shown in brown with non-carbon atoms colored by type. The $2F_o - F_c$ electron density map is contoured to 1.0σ and shown as a gray mesh, and zinc ions are shown as gray spheres. Hydrogen bonds, zinc coordination bonds, and hydrophobic interactions are shown as thin black, thin blue, and thick gray dashes, respectively.

intercalated S1 presumably decreases the electrostatic repulsion between the two zinc ions. Polarizable molecular mechanics studies support this intercalation scheme as being the most energetically favorable mode of binding and suggest that the S1 sulfhydryl exists as an anion, similar to the catalytic hydroxide. This is due to the effect of zinc in lowering the pK_a of bound thiol groups by ~2 orders of magnitude.[21]

L-Captopril presents two binding faces, a hydrophobic face that interacts with the L3 loop and a hydrophilic face that hydrogen-bonds to N220 on the L10 loop. A hydrogen-bonding interaction exists between the N220 backbone amide and the L-captopril O2 at 3.3 Å (Figure S6). In addition, hydrophobic contacts exist between the L3 loop residues V73 and M67 and the L-captopril C6 and C3 atoms and between the L5 loop residue W93 and the L-captopril C3 and C5 atoms (Figure 3B).

Interestingly, an overlay of the BlaB-bound D-captopril structure[6] and our NDM-1-bound L-captopril structure reveals that the two diastereomers bind in opposite orientations yet

intercalate their S1 atoms in exactly the same fashion (Figure S3). These two enzymes share 26% sequence identity yet contain very similar active-site architectures and virtually identical zinc coordination geometries. On this basis, it has been suggested that D-captopril likely adopts the same general orientation within the BlaB and NDM-1 active sites.[21] Indeed, NDM-1 contains many potential hydrogen-bond donors and acceptors capable of making productive contacts with D-captopril in the BlaB-type orientation (Figure S3). The K_i values for inhibition of NDM-1-mediated imipenem hydrolysis by D- and L-captopril are 1.3 and 39.0 μM, respectively.[17,22] The fact that the two high-affinity diasteriomers are capable of making productive contacts and display virtually identical S1 zinc intercalation suggests that a fusion of the two molecules whereby D- and L-captopril share a common S1 and C1 may generate an even more tightly binding inhibitor.

Despite having relatively low sequence identity, the class-B1 MBLs in general display remarkable structural similarity, especially with respect to the disposition of the catalytic residues and ions.[3] Consequently, inhibitory compounds often act universally on all MBLs. Sulfhydryl-mediated zinc intercalation is emerging as an exciting avenue for the development of competitive MBL inhibitors.[5,6] Our L-captopril-bound structure lends further support to this approach and presents possible ways to increase the binding affinity. An alternative approach for overcoming MBL resistance would be to design β-lactam antibiotics that are not recognized by MBLs. Our product complex structures reveal that the traditional strategy of developing newly functionalized R1 and R2 groups may be readily thwarted by the plastic and open nature of the MBL active site. However, the monobactam core provides a promising scaffold on which to synthesize novel MBL-resistant β-lactams.

■ ASSOCIATED CONTENT

Ⓢ Supporting Information

Procedures for protein expression and purification, crystallization, data collection, and structure determination; table of crystallographic data; table of crystallographic parameters and refinement statistics; figures showing ligand binding distances; and CIF and PDB files. This material is available free of charge via the Internet at http://pubs.acs.org.

■ AUTHOR INFORMATION

Corresponding Author
natalie@byron.biochem.ubc.ca

Notes
The authors declare no competing financial interest.

■ ACKNOWLEDGMENTS

■ REFERENCES

(1) Dalhoff, A.; Thomson, C. J. *Int. J. Exp. Clin. Chemother.* **2003**, *49*, 105.

(2) Suavage, E.; Kerff, F.; Terrak, M.; Ayala, J. A.; Charlier, P. *FEMS Microbiol. Rev.* **2008**, *32*, 234.

(3) Bebrone, C. *Biochem. Pharmacol.* **2007**, *74*, 1686.

(4) Wang, Z.; Fast, W.; Valentine, A. M.; Benkovic, S. J. *Curr. Opin. Chem. Biol.* **1999**, *3*, 614.

(5) Drawz, S. M.; Bonomo, R. A. *Clin. Microbiol. Rev.* **2010**, *23*, 160.

(6) García-Sáez, I.; Hopkins, J.; Papamicael, C.; Franceschini, N.; Amicosante, G.; Rossoline, G. M.; Galleni, M.; Frère, J. M.; Dideberg, O. *J. Biol. Chem.* **2003**, *278*, 23868.

(7) Kumarasamy, K. K.; Toleman, M. A.; Walsh, T. R.; Bagaria, J.; Butt, F.; Balakrishnan, R.; Chaudhary, U.; Doumith, M.; Giske, C. G.; Irfan, S.; Krishnan, P.; Kumar, A. V.; Maharjan, S.; Mushtaq, S.; Noorie, T.; Paterson, D. L.; Pearson, A.; Perry, C.; Pike, R.; Rao, B.; Ray, U.; Sarma, J. B.; Sharma, M.; Sheridan, E.; Thirunarayan, M. A.; Turton, J.; Upadhyay, S.; Warner, M.; Welfare, W.; Livermore, D. M.; Woodford, N. *Lancet Infect. Dis.* **2010**, *10*, 597.

(8) Schneider, K. D.; Karpens, M. E.; Bonomo, R. A.; Leonard, D. A.; Powers, R. A. *Biochemistry* **2009**, *48*, 11840.

(9) McKenna, M. *Sci. Am.* **2011**, *304*, 46.

(10) Hsu, L. Y.; Koh, T. H. *Singapore Med. J.* **2011**, *52*, 230.

(11) Zhang, H.; Hao, Q. *FASEB J.* **2011**, *2*, 1.

(12) King, D.; Strynadka, N. *Protein Sci.* **2011**, *20*, 1484.

(13) Concha, N. O.; Rasmussen, B. A.; Bush, K.; Herzberg, O. *Structure* **1996**, *4*, 823.

(14) Park, H.; Brothers, E. N.; Merz, K. M. *J. Am. Chem. Soc.* **2005**, *127*, 4232.

(15) Yang, H.; Aitha, M.; Hetrick, A. M.; Richmond, T. K.; Tierney, D. L.; Crowder, M. W. *Biochemistry* **2012**, *51*, 3839.

(16) Han, S.; Zaniewski, R. P.; Marr, E. S.; Lacey, B. M.; Tomaras, A. P.; Evdokimov, A.; Miller, J. R.; Shanmugasundaram, V. *Proc. Natl. Acad. Sci. U.S.A.* **2010**, *107*, 22002.

(17) Yong, D.; Toleman, M. A.; Giske, C. G.; Cho, H. S.; Sundman, K.; Lee, K.; Walsh, T. R. *Antimicrob. Agents Chemother.* **2009**, *53*, 5046.

(18) Auld, D. S. *BioMetals* **2001**, *14*, 271.

(19) Brown, N. G.; Horton, L. B.; Huang, W.; Vongpunsawad, S.; Palzkill, T. *Antimicrob. Agents Chemother.* **2011**, *55*, 5696.

(20) Materon, I. C.; Beharry, Z.; Huang, W.; Perez, C.; Palzkill, T. *J. Mol. Biol.* **2004**, *344*, 653.

(21) Antony, J.; Gresh, N.; Olsen, L.; Hemmingsen, L.; Schofield, C. J.; Bauer, R. *J. Comput. Chem.* **2002**, *23*, 1281.

(22) Guo, Y.; Wang, J.; Niu, G.; Shui, W.; Sun, Y.; Zhou, H.; Zhang, Y.; Yang, C.; Lou, Z.; Rao, Z. *Protein Cell* **2011**, *2*, 384.